AFRL-RH-WP-TR-2016-0086

HOST- HIF-1α PATHWAY AND HYPOXIA: *IN VITRO* STUDIES AND MATHEMATICAL MODEL

Peter J. Robinson
Molly E. Chapleau
Elaine A. Merrill
Meghan K. Makley
R. Arden James

Henry M. Jackson Foundation
For the Advancement of Military Medicine
Wright-Patterson AFB OH

Kyung O. Yu
Deirdre A. Mahle
David R. Mattie

Bioeffects Division
Molecular Bioeffects Branch

August 2016

Molecular Bioeffects Branch
Bioeffects Division
Airmen Systems Directorate
711th Human Performance Wing
Air Force Research Laboratory
Wright-Patterson AFB OH 45433-5707

NOTICE AND SIGNATURE PAGE

Using Government drawings, specifications, or other data included in this document for any purpose other than Government procurement does not in any way obligate the U.S. Government. The fact that the Government formulated or supplied the drawings, specifications, or other data does not license the holder or any other person or corporation; or convey any rights or permission to manufacture, use, or sell any patented invention that may relate to them.

Qualified requestors may obtain copies of this report from the Defense Technical Information Center (DTIC) (http://www.dtic.mil).

The experiments reported were conducted according to the "Guide for the Care and Use of Laboratory Animals," Institute of Laboratory Animal Resources, National Research Council.

(AFRL-RH-WP-TR - 2016 - 0086) has been reviewed and is approved for publication in accordance with assigned distribution statement.

MATTIE.DAVID.R.1230101880

Digitally signed by MATTIE.DAVID.R.1230101880
DN: c=US, o=U.S. Government, ou=DoD, ou=PKI, ou=USAF, cn=MATTIE.DAVID.R.1230101880
Date: 2016.11.28 12:52:33 -05'00'

DAVID R. MATTIE, Work Unit Manager
Molecular Bioeffects Branch

POLHAMUS.GARRETT.D.1175839484

Digitally signed by POLHAMUS.GARRETT.D.1175839484
DN: c=US, o=U.S. Government, ou=DoD, ou=PKI, ou=USAF, cn=POLHAMUS.GARRETT.D.1175839484
Date: 2016.11.28 13:57:27 -06'00'

GARRETT D. POLHAMUS, DR-IV, DAF
Chief, Bioeffects Division
Human Effectiveness Directorate
711th Human Performance Wing
Air Force Research Laboratory

This report is published in the interest of scientific and technical information exchange, and its publication does not constitute the Government’s approval or disapproval of its ideas or findings.

REPORT DOCUMENTATION PAGE

Form Approved
OMB No. 0704-0188

1. REPORT DATE *(DD-MM-YYYY)*	2. REPORT TYPE	3. DATES COVERED *(From - To)*
08-30-2016	Interim	Oct 2014 – Mar 2016

4. TITLE AND SUBTITLE
Host - HIF-1α Pathway and Hypoxia: *In Vitro* Studies and Mathematical Model

5a. CONTRACT NUMBER
In-House

5b. GRANT NUMBER
NA

5c. PROGRAM ELEMENT NUMBER
62202F

6. AUTHOR(S)
Robinson, Peter J.[1], Molly E. Chapleau[1], Elaine A. Merrill[1], Meghan K. Makley[1], R. Arden James[1], Kyung O. Yu[*], Deirdre A. Mahle* and David R. Mattie.*

5d. PROJECT NUMBER
7757

5e. TASK NUMBER
HD

5f. WORK UNIT NUMBER
05/H0D1

7. PERFORMING ORGANIZATION NAME(S) AND ADDRESS(ES)
[1]HJF, 2728 Q St, Bldg 837, WPAFB OH 45433-5707

8. PERFORMING ORGANIZATION REPORT NUMBER

9. SPONSORING/MONITORING AGENCY NAME(S) AND ADDRESS(ES)
Air Force Materiel Command*
Air Force Research Laboratory
711th Human Performance Wing
Human Effectiveness Directorate
Bioeffects Division
Molecular Bioeffects Branch
Wright-Patterson AFB OH 45433-5707

10. SPONSOR/MONITOR'S ACRONYM(S)
711 HPW/RHDJ

11. SPONSORING/MONITORING AGENCY REPORT NUMBER
AFRL-RH-WP-TR-2016-0086

12. DISTRIBUTION AVAILABILITY STATEMENT
Distribution A: Approved for public release; distribution unlimited. (PA Case No. 88ABW-2016-6146, 1 Dec 2016)

13. SUPPLEMENTARY NOTES

14. ABSTRACT
Episodes of hypoxia were implicated in F-22 pilots after training missions in which questions about pilot exposures and mission accomplishment were raised. These episodes identified data gaps in the understanding the complexities of exposures to pilots in high performance aircraft including variations in oxygen availability and physiological usage was in question. We therefore undertook a project need to understand how hypoxia relates to alterations in brain functioning. Responses to hypoxia take place at multiple levels. The initial response is through the carotid body altering physiology (breathing, blood flow). Tissue level responses involve regulating demand for oxygen through altered function. Key to understanding these responses both at the physiological and tissue (brain) level are oxygen sensing pathways, particularly those involving HIF-1α. These linked pathways need to be understood mechanistically and quantitatively. *In vitro* studies are useful for elucidating elements of these processes. These changes in complex pathways need to be integrated and applied (extrapolated) to relevant human exposure scenarios in order to assess the relevance of hypoxia occurrences into the abovementioned AF issues. A mathematical model was developed integratinge these experimental measurements thatand provides an initial description of the mechanisms of hypoxia and the organism's response. The initial iteration of our model focuses on the brain. It includes delivery of oxygen to the cell, and the response of the HIF-1α signaling pathway in terms of alterations in gene expression.

15. SUBJECT TERMS
mathematical model, signaling pathways, hypoxia, immunohistochemistry, ELISA, inhalation chamber

16. SECURITY CLASSIFICATION OF:			17. LIMITATION OF ABSTRACT	18. NUMBER OF PAGES	19a. NAME OF RESPONSIBLE PERSON
U					D.R. Mattie
a. REPORT	b. ABSTRACT	c. THIS PAGE	SAR	38	19b. TELEPONE NUMBER (*Include area code*)
U	U	U			NA

Standard Form 298 (Rev. 8-98)
Prescribed by ANSI-Std Z39-18

THIS PAGE INTENTIONALLY LEFT BLANK.

TABLE OF CONTENTS

LIST OF FIGURES

PREFACE

Funding for this project was provided through the Aerospace Toxicology Program, which is part of the Aerospace Physiology and Toxicology Program in the 711 Human Performance Wing of the Air Force Research Laboratory. This research was conducted under cooperative agreements FA8650-10-2-6062 and FA8650-15-2-6608, both with the Henry M. Jackson Foundation for the Advancement of Military Medicine (HJF). The program manager for the HJF cooperative agreements was David R. Mattie, PhD (711 HPW/RHDJ), who was also the technical manager for this project.

The authors also would like to acknowledge Laura K. Braydich-Stolle of HJF (Wright-Patterson AFB OH) for her contributions to the content of this technical report, Teresa R. Sterner of HJF for formatting this technical report for submission, and Michael Ray (AFRL/RQQE, Wright-Patterson AFB OH) for invaluable work in the construction of the chambers in Section 3.2.

THIS PAGE INTENTIONALLY LEFT BLANK.

1.0 SUMMARY

Episodes of hypoxia-like events experienced by F-22 pilots after training missions have raised questions about pilot exposures and mission accomplishment. These episodes identified data gaps in the understanding of pilot exposures in high performance aircraft. We, therefore, need to understand how levels of low oxygen at lower than atmospheric pressure causes physiological hypoxia, and how this relates to alterations in cognition.

Responses to hypoxia take place at multiple levels within the human body. The initial response is through the carotid body altering physiology (breathing, blood flow). Tissue level responses involve regulating demand for oxygen through altered function. Key to understanding these responses both at the physiological and tissue (brain) level are oxygen sensing pathways, particularly those involving the oxygen sensing cytosolic gene transcription factor HIF-1α. These linked pathways need to be understood mechanistically and quantitatively.

In vitro studies are useful for elucidating elements of these processes. These need to be integrated and applied (extrapolated) to relevant human exposure scenarios in order to assess the relevance of hypoxia to the abovementioned Air Force issues.

A mathematical model was developed to integrate these experimental measurements and provide a description of the mechanisms of hypoxia and the organism's response. The initial iteration of our model focuses on the brain. It includes delivery of oxygen to the cell, and the response of the HIF-1α signaling pathway in terms of alterations in gene expression.

2.0 INTRODUCTION

Episodes of hypoxia-like events experienced by F-22 pilots after training missions have raised questions about pilot exposures and mission safety during sortie accomplishment (Martin *et al.*, 2012). These episodes identified data gaps in the understanding of exposures to pilots in high performance aircraft. We therefore need to understand how hypoxia relates to alterations in brain functioning. Responses to hypoxia take place at multiple levels. The initial response is through carotid body altering physiology (breathing, blood flow). Tissue level responses involve regulating demand for oxygen through altered function. Key to understanding these responses both at the physiological and tissue (brain) level are oxygen sensing pathways, particularly those involving hypoxia inducible factor 1-alpha (HIF-1α). These linked pathways need to be understood mechanistically and quantitatively. *In vitro* studies are useful for elucidating elements of these processes. These results from cultured cellular systems need to be integrated and applied (extrapolated) to relevant human exposure scenarios in order to assess the relevance of hypoxia to the abovementioned Air Force issues.

Compensatory mechanisms for hypoxia in brain (and other tissues) work at a number of time scales and include physiological and cellular responses. Physiological responses are fast-acting and prevent cellular hypoxia (within limits). These are typically mediated by the carotid and aortic bodies, which are sensory organs for detecting changes in arterial blood due to increased CO_2 or decreased O_2 levels. Systemic cardiac, vascular and respiratory responses to hypoxia are mediated via afferent nerves that carry signals back from the carotid and aortic bodies to the brainstem, which responds accordingly by, for example, increasing the ventilation rate.

Responsiveness of the carotid body (CB) to acute hypoxia relies on the inhibition of O_2 sensitive K^+ channels in glomus cells, which leads to cell depolarization, Ca^{2+} entry and release of transmitters that activate afferent nerve fibers; the molecular mechanisms underlying K^+ channel modulation by O_2 tension may involve disruption of the prolyl hydroxylase/hypoxia inducible factor pathway (Lopez-Barneo *et al.*, 2008). Evidence that HIF-1α is involved with carotid body responses to hypoxia includes studies with HIF-1α +/- mice (Kline *et al.*, 2002; Peng *et al.*, 2006), in which the hypoxia response was severely impaired. However, it is unlikely that acute responses to hypoxia by the carotid body (such as regulation of breathing and heart rate) are mediated by the HIF-1α pathway (Wyatt, personal communication.).

When such first tier, physiological protection mechanisms are inadequate, cellular hypoxia ensues, and affected cells such as neurons adapt to the hypoxic conditions by altering gene-regulated cellular processes such as metabolism, apoptosis, angiogenesis, and cell proliferation and differentiation. Figure 1 illustrates this two tiered adaptive response to hypoxia.

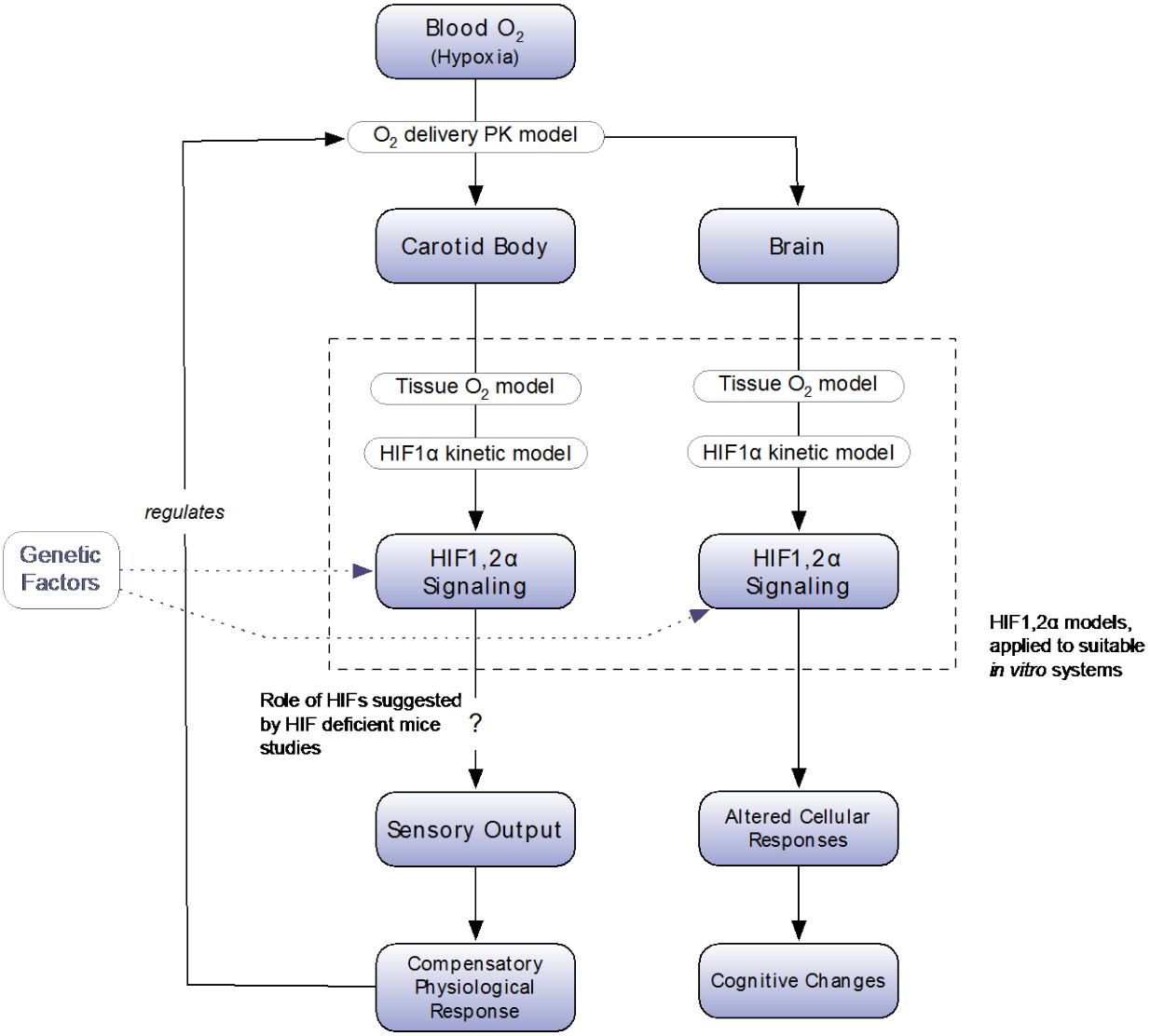

Figure 1. Schematic of the Physiological Response to Hypoxia via the Carotid Body. The carotid body, together with the tissue response to hypoxia, are both mediated by the HIF-1α signaling pathway.

In both the carotid bodies (Prabhakar, 2013), and other tissues, therefore, the primary sensing mechanism involves the build-up of HIF-1α transcription factor protein. The presence of oxygen activates hydroxylases (such as prolyl hydroxylase, PHD) to hydroxylate HIF-1α, allowing the von Hippel-Lindau tumor suppressor protein (VHL) to bind, leading to HIF-1α ubiquitination and degradation (Figure 2). Under low oxygen conditions, hydroxylase inactivity allows HIF-1α protein to accumulate, and binding of p300/cAMP response element binding protein (CBP) cofactors facilitates translocation to the nucleus and subsequent gene transcription. HIF-1α dimerizes with HIF-1β and translocates to the nucleus where it associates with CBP and DNA polymerase II and then binds DNA to initiate transcription, up-regulating expression of apoptotic, angiogenic, erythropoeitic, and other proteins (see Section 5.3).

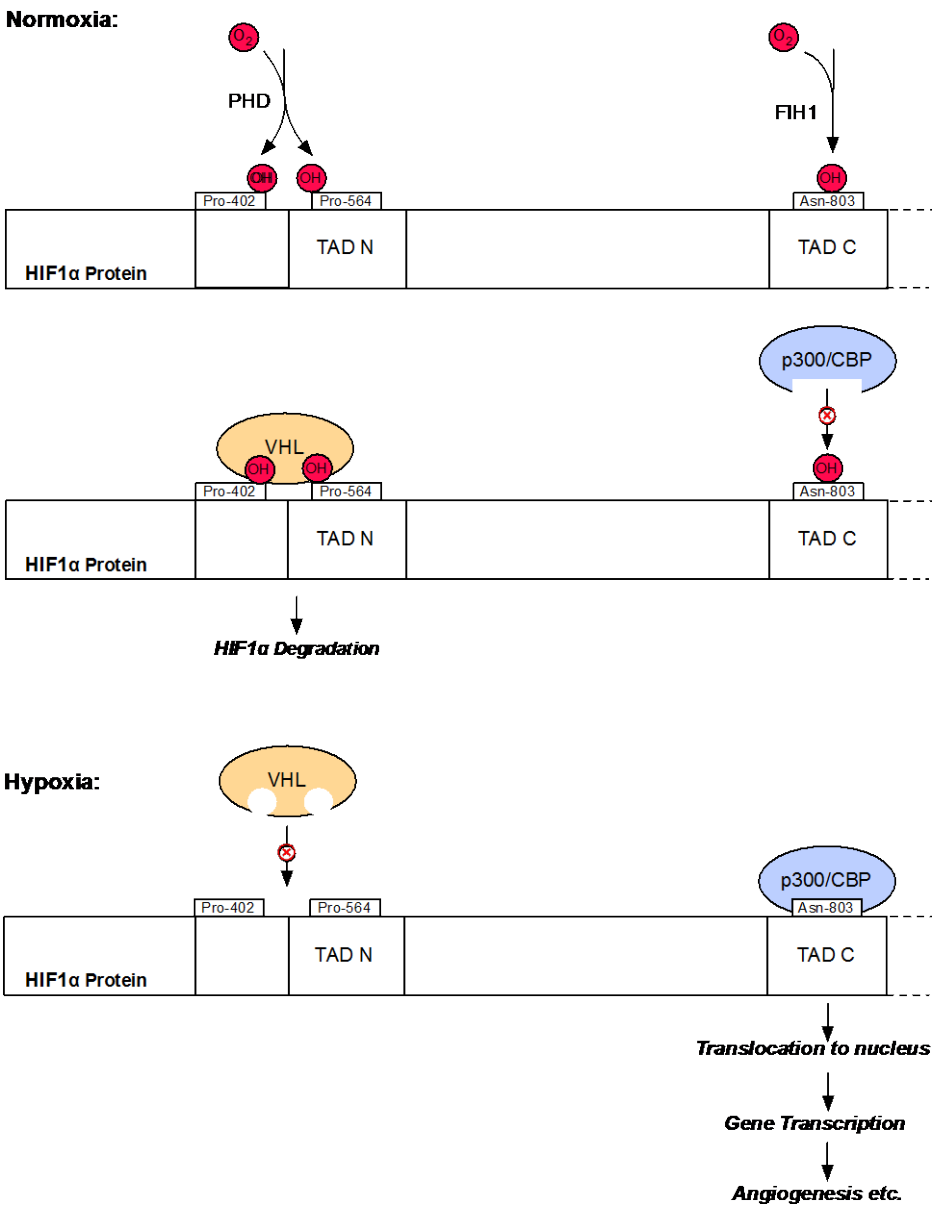

Figure 2. Binding Sites on HIF-1α Protein. N- and C-terminal transactivation domains (TAD N and TAD C) are regions for HIF-1α degradation and transcriptional activation, respectively. Under normoxic conditions, hydroxylation of Pro-402 and Pro-564 by the HIF-1α prolyl hydroxylases (PHD) allows the von Hippel-Lindau tumor suppressor protein (VHL) to bind, which permits HIF-1α ubiquitination and degradation, maintaining low levels of HIF-1α in the cytosol. At the same time, hydroxylation of Asn-803 by factor inhibiting HIF-1 (FIH1) prevents the interaction of HIF-1α with the cofactors p300 and CBP (CREB binding protein). Under hypoxic conditions, hydroxylation is less likely, VHL does not bind and HIF-1α builds up in the cytosol. At the same time, binding of p300/CBP cofactors facilitates translocation to the nucleus and subsequent gene transcription. (Adapted from Semenza, 2004).

The model can be extended to include a gene transcription signal and gene transcription itself as output from the HIF-1α pathway. In such an extended model, the output from the current model (HIF-1α binding to hypoxia responsive element (HRE) and the resulting transcription signal) would provide an input to a model of gene expression, such as one provided by Chen *et al.* (1999) or Ay *et al.* (2011), thereby linking to angiogenesis and finally to alterations in capillary density (LaManna *et al.*, 2004) (see Section 5.0 below).

In addition to hypoxic conditions, ambient pressures and air quality also can add to the impact of hypoxia on physiological responses. In many cases oxygen delivery issues occur concurrently with novel chemical and chemical mixture exposure issues. For example, toluene is known to come through the aircraft's on-board oxygen generation system (OBOGS), and has been one of the most prevalent chemicals seen in analyses of USAF aircraft and cockpit locations (Martin *et al.*, 2012). Toluene may impact oxygen delivery to tissues by binding to hemoglobin, potentially altering its oxygen carrying capacity (Chushak *et al.*, 2015).

A number of experimental studies can be conducted to elucidate the mechanisms associated with both the physiological and cellular responses to hypoxia. *In vivo* studies can be used to explore the physiological responses mediated by the carotid body. In addition, there is the possibility of looking at HIF signaling in cultured Type 1 carotid bodies. In general, *in vitro* studies can be used to study hypoxia responses in specific cell types, such as neurons. For example, high-throughput *in vitro* screening can be used to monitor expression of HIF-1α, determine proteomic profiles of hypoxic events and identify potential protein markers for further investigation during *in vivo* studies. Immunohistochemical staining (IHC) of whole brain from altitude studies would identify regions most affected by hypoxia. A HIF-1α specific antibody can be used to find cytosolic and nuclear accumulation of HIF-1α. Protein biomarkers identified from *in vitro* studies can also be evaluated by IHC. IHC also allows localization of HIF-1α within the cell, specifically its translocation to the nucleus prior to gene transcription. Finally, it is also possible to measure mRNA levels of relevant proteins in the hypoxia signaling pathways.

3.0 METHODS

3.1 *In Vitro* Cobalt Chloride Methods

This report describes three related approaches to understanding the role of the HIF-1α pathway in the physiological responses to hypoxia. Firstly, *in vitro* experiments with NE-4C, Neuro-2a (N2a), C8-B4, and SK-N-SH cells are described, in which hypoxia is simulated with cobalt chloride ($CoCl_2$) exposure. $CoCl_2$ acts as a hypoxia surrogate by binding to HIF-1α, thereby inhibiting its interaction with VHL and preventing HIF-1α degradation (Yuan *et al.*, 2003). HIF-1α activation and localization was measured by an enzyme-linked immunosorbent assay (ELISA) and IHC techniques. Secondly, an atmospheric exposure chamber was designed and developed that allowed the creation of hypoxic exposure conditions for tissue culture models, and HIF-1α induction was measured using ELISA. Finally, a mathematical model was developed to describe the HIF-1α pathway's role in the cellular and physiological responses to hypoxia,

with a future aim to integrate *in vitro* studies and extrapolate to and understand the role of HIF-1α in *in vivo* situations.

3.1.1 Cell Culture Lines and Methods. NE-4C mouse embryonic neuroectodermal stem cells, N2a mouse neuroblastoma cells, C8-B4 transformed mouse cerebellum microglial cells, and SK-N-SH human neuroblastoma cells were obtained from the American Type Culture Collection (ATCC, Manassas VA). These cell types were chosen because they express HIF-1α; in addition the NE-4C, N2a, and SK-N-SH cells represent neuronal cells, while the C8-B4 cells represent microglia, another important cell type in the brain. NE-4C cells were cultured on Primaria™ plates (Corning™, Corning NY) in Eagle's Minimum Essential Medium (EMEM, ATCC) supplemented with 10 percent heat-inactivated fetal bovine serum (FBS, ATCC) and 4 mM L-glutamine (Sigma-Aldrich, St. Louis MO). N2a, C8-B4 and SK-N-SH cells were cultured in EMEM supplemented with 10 percent FBS. N2a and SK-N-SH cells were cultured in uncoated tissue culture flasks (Corning), and C8-B4 cells were cultured in poly-D-lysine-coated BioCoat flasks (BD Biosciences, San Jose CA). Before seeding, cells were washed with phosphate buffered saline (PBS), pH 7.4 (Gibco, part of ThermoFisher Scientific, Waltham MA), trypsinized with 0.25 percent trypsin-ethylenediaminetetraacetic acid (EDTA, ATCC), and collected and counted using trypan blue (Invitrogen, part of ThermoFisher Scientific) on a Countess automated cell counter (Invitrogen).

3.1.2 Cobalt Chloride Exposures - HIF-1α ELISA. Cobalt chloride ($CoCl_2$, Alfa Aesar, part of ThermoFisher Scientific) was used as a hypoxia mimetic to activate the HIF-1α transcription factor in four cell lines of interest (NE-4C, N2a, C8-B4 and SK-N-SH). Exposure to 250µM $CoCl_2$ was accomplished in T75 flasks or 100 mm Primaria™ plates. T75 flasks of N2a, C8-B4 and SK-N-SH cells were seeded at 1:3 or 1:4 ratio. Primaria™ plates (100 mm) and were seeded with NE-4C cells at 1:10 ratio. All subcultures were grown to approximately 80 to 90 percent confluence at 37°C in 5 percent CO_2 atmosphere. Hypoxic cell response was induced by incubation of cells with 250 µM $CoCl_2$ for 24 hours. A 15 mM stock solution of $CoCl_2$ was prepared by dissolving 71.2 mg of chemical in 20 mL of water. Stock $CoCl_2$ solution was added to fresh complete medium in culture flasks and cells were incubated at 37°C with 5 percent CO_2 for approximately 24 hours. Control cultures were dosed with equivalent volumes of sterile PBS and otherwise treated identically to hypoxic cultures.

3.1.3 Cobalt Chloride Exposures – Immunocytochemistry. Exposure to concentrations of $CoCl_2$ ranging from 150 µM to 1 mM were accomplished in 96-well imaging plates (BD Falcon™, BD Biosciences). Cells were seeded at 35,000 viable cells/well in uncoated (N2a, SK-N-SH, C8-B4) or poly-D-lysine-coated (NE-4C) wells. Cells were incubated at 37°C in 5 percent CO_2 atmosphere overnight to allow them to adhere before initiating $CoCl_2$ exposures. Hypoxic cell response was induced by incubation of cells in 75 µL of complete growth medium containing 0, 150, 250, 500, 750, or 1000 µM $CoCl_2$ for 24 hours at 37°C in 5 percent CO_2. Dosing medium was prepared by adding 15 mM $CoCl_2$ stock solution to complete medium. The dosing medium was then gently added to wells containing cell monolayers, using cut-off pipet

tips to decrease monolayer disruption. Plates were placed in a 37°C incubator with 5 percent CO_2 for 24 hours.

3.1.4 HIF-1α Detection – ELISA. After 24 hours of exposure to PBS or $CoCl_2$, flasks were removed from the incubator and briefly observed under the microscope for general morphology, viability, and adhesion assessment. Floating and adherent cells were collected together by scraping to remove adherent cells and transferring all of the medium and cells to a centrifuge tube. Medium was centrifuged at 300 x g for 5 minutes at 4°C to collect cells. Cells were washed twice with 1 mL of sterile PBS. Cell pellets were then solubilized ($1x10^7$ cells/mL) by addition of Lysis Buffer #11 (R&D Systems, Inc., Minneapolis MN), and mixed by re-suspending through vortexing and then incubated on ice for 30 minutes. Lysates were clarified by centrifugation at 2000 x g for 5 minutes at 4°C. Supernatant was transferred to a clean tube and stored at -70°C or below until ready to perform the ELISA. HIF-1α ELISA (R&D Systems) was performed according to manufacturer's protocol.

3.1.5 HIF-1α Detection – Immunocytochemistry. After 24 hours of exposure to $CoCl_2$, cell culture imaging plates were removed from the incubator and cells were briefly observed under the microscope for general morphology, viability and adhesion assessment. Dosing medium was gently removed from all wells using cut-off pipet tips. (Note that cut-off pipet tips were used throughout this protocol to prevent disruption of cell monolayer.) Cells were washed once with PBS, pH 7.4, and fixed for 20 minutes in 2 percent paraformaldehyde (Electron Microscopy Sciences (EMS), Hatfield PA) in PBS at room temperature. Cells were washed twice with PBS, then permeabilized for 10 minutes in 0.1 percent Triton X-100 (Sigma-Aldrich) in PBS. Cells were washed twice with PBS, then blocked for 1 hour in 10 percent horse serum (ATCC) in PBS-Triton X-100. Blocking buffer was removed and cells were incubated with primary HIF-1α antibody (SC-53546, Santa Cruz Biotechnology, Dallas TX) diluted 1:250 in blocking buffer for 1 hour at 37°C. Cells were washed twice with PBS. Cells were incubated in blocking buffer containing secondary antibody diluted 1:250 (SC-2010, Santa Cruz Biotechnology) and 1 µL/mL Hoechst® 33342 dye (ThermoFisher Scientific, formerly Life Technologies) for 1 hour at room temperature in the dark. Secondary antibody solution was removed and cells were washed twice with PBS, avoiding direct light. Fifty µL of PBS was added to each well, and cells were observed and imaged on an Olympus Fluoview 1000 laser confocal microscope.

3.2 *In Vitro* Hypoxia (diminished oxygen atmosphere) Studies

3.2.1 Hypoxia Chamber Design. This section describes the design and development of a custom made glass chamber to create hypoxic exposure conditions for tissue culture models. Expression of HIF-1α, was used as a biomarker to confirm exposure.

A 7 inches wide by 6 inches high custom blown, constructed glass chamber that can hold tissue culture plates was designed for vapor exposures (Figure 3A). Previous atmosphere distribution testing established a flow path represented by the schematic in Figure 3B (Yu *et al.*, 2015).

When a polystyrene 24-well plate with cells was exposed to gas or vapor, cells adhered on the bottom of the well were not exposed to vapor due to a liquid barrier created by the media which caused slow equilibrium diffusion between the media and gas phase. Figure 3C illustrates gas exchange in a traditional tissue culture vessel. In comparison, gas exchange can easily occur across a thin film in the lumox® plates (Sarstedt AG & Co., Numbrecht, Germany) (Figure 3D).

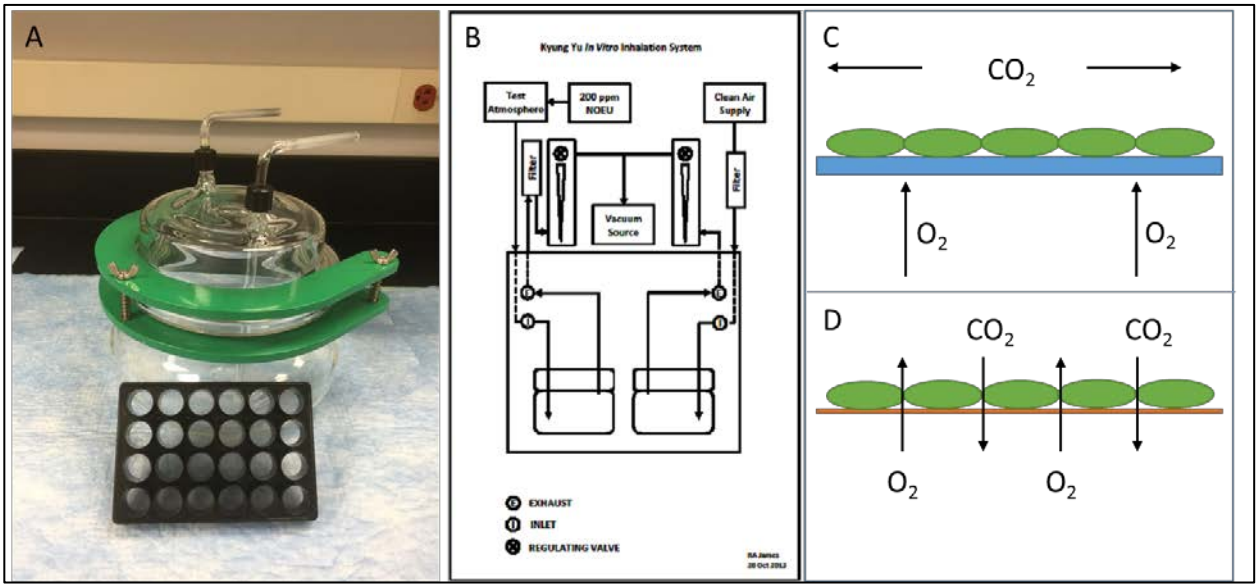

Figure 3. Hypoxia Chamber. A) The lumox® 24-well plate in front of custom-made glass chamber. Chamber dimensions are 7 inches wide by 6 inches high. B) Air flow schematic for the glass chamber. C) Gas exchange pattern in a traditional cell culture plate D) Gas exchange pattern for the lumox® plates.

Using this novel chamber design, three human cell lines were used: A549 adenocarcinomic alveolar basal epithelial cells (ATCC), HaCaT transformed aneuploid immortal keratinocyte cells (generously donated by the U.S. Army Medical Research Institute of Chemical Defense, Aberdeen Proving Ground MD), and SK-N-SH neuroblastoma cells (ATCC). A549 cells were grown at 37°C in a humidified incubator using RPMI-1640 medium (Life Technologies, Carlsbad, CA) supplemented with 10 percent heat inactivated FBS (Life Technologies) and one percent Pen-Strep (ATCC; 10,000 units penicillin, 10 mg streptomycin in 0.9% NaCl). HaCaT cells were grown at 37°C in a humidified incubator using RPMI-1640 medium supplemented with 10 percent FBS (ATCC) and one percent Pen-Strep. The cells were chosen because they express HIF-1α; in addition the SK-N-SH cells represent human neuronal cells, while the A549 cells represent lung alveolar cells, whose response to hypoxia is also of interest. The cells were seeded at 500K/well on the lumox® 24-well plates and exposed for two hours to air as a control or 1 percent O_2 (in N_2) to simulate hypoxic conditions (Figure 4). The exposure chamber was placed inside of an incubator chamber wherein temperature was maintained at 37°C.

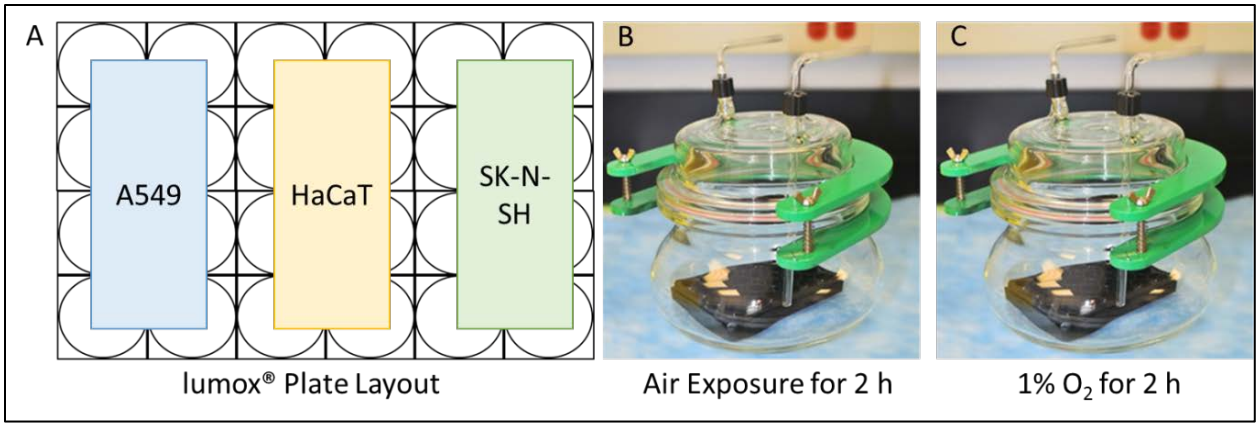

Figure 4. **Cell Exposure Experimental Design.** A) Layout of lumox® 24-well plates with cell lines; B) Chamber for control exposures; C) Chamber for hypoxia exposures

3.2.2 Validation of Hypoxic Exposure In Vitro. Following exposure to the different atmospheric conditions, protein was extracted from the cells. For a detailed protocol about the cell scraping and lysis procedure see Appendix A. The protein extracts were processed with the HIF-1α ELISA kit (Human/Mouse Total HIF-1α ELISA, R&D Systems) to quantify changes in expression. Appendix B describes the optimized protocol for the HIF-1α ELISA procedure.

3.3 HIF-1α Mathematical Model for Brain

A mathematical model was developed to integrate these experimental measurements and provide a description of the mechanisms of hypoxia and the organism's response. One advantage of developing such a model is that it permits extrapolation to different exposure conditions. The data obtained for hypoxia *in vitro* is usually based on exposure periods on the order of hours. Real-life exposures to pilots may be of much shorter duration (often seconds to minutes), while longer term effects involving gene transcription, such as angiogenesis, may develop over much longer periods of time (days to weeks). The response of the HIF-1α pathway to changes in intracellular O_2 is rapid, and our model reflects this. In addition, our model ultimately will be linked to gene transcription events, and so will also be able to describe longer-term sequelae (see *Conclusions and Future Work* below).

The initial iteration of our model focuses on the brain. It includes delivery of oxygen to the cell, and the response of the HIF-1α signaling pathway in terms of alterations in gene expression (Figure 5; which also shows the potential interaction of toluene with oxygen delivery).

The mechanism underlying the HIF-1α pathway has been described in Section 2.0. The essential processes that are implemented in our model are as follows:

- Diffusion of O_2 into the intracellular space
- Hydroxylation of HIF-1α by PHD (and binding of VHL), leading to HIF-1α degradation

- Under low oxygen conditions, hydroxylase inactivity allows HIF-1α protein to accumulate in the cytosol
- Translocation of HIF-1α to the nucleus, and
- Binding to HRE on the DNA, and subsequent gene transcription.

These processes are represented schematically in Figure 6. Our model is necessarily simplified. Our aim is to capture the essential behavior of the system in a way that relates to the available experimental data. Our initial model is largely unparameterized, and initial assumptions are made to form parameter values in order to elicit appropriate model behavior. As experimental data is incorporated into the model, these parameter values will be updated and refined in an iterative manner.

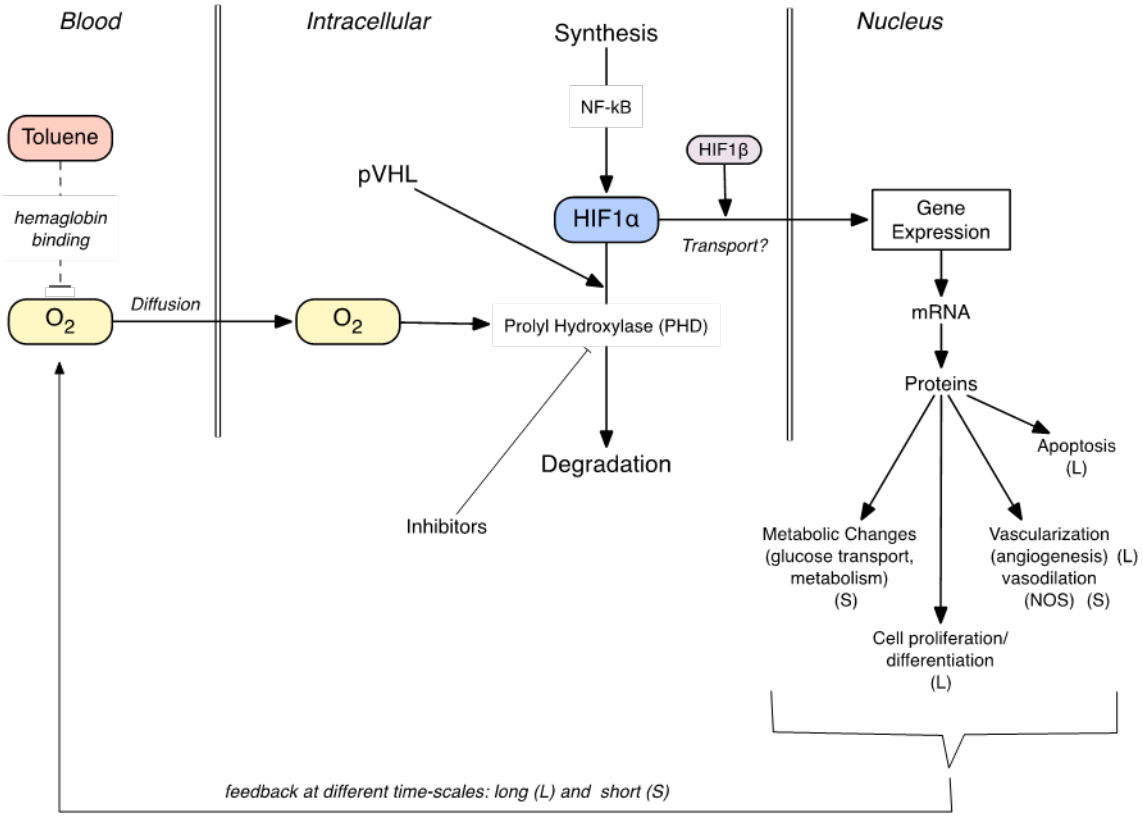

Figure 5. Schematic of the HIF-1α Pathway in Cells. Cells such as neurons respond to cellular hypoxia by altering gene expression. Key processes (from left to right in the figure) include: diffusion of O_2 into the intracellular space; hydroxylation of HIF-1α by prolyl hydroxylase, PHD (and binding of Hippel-Lindau tumor suppressor protein (VHL), leading to HIF-1α degradation; accumulation of HIF-1α protein in the cytosol under hypoxic conditions; translocation of HIF-1α to the nucleus; binding to hypoxia responsive element (HRE) on the DNA, and subsequent gene transcription resulting in short-term (S) and longer term (L) adaptation (lower right). Toluene (top left) potentially interacts with this process by binding to hemoglobin in the blood, reducing oxygen transport to tissues (Chushak *et al.*, 2015).

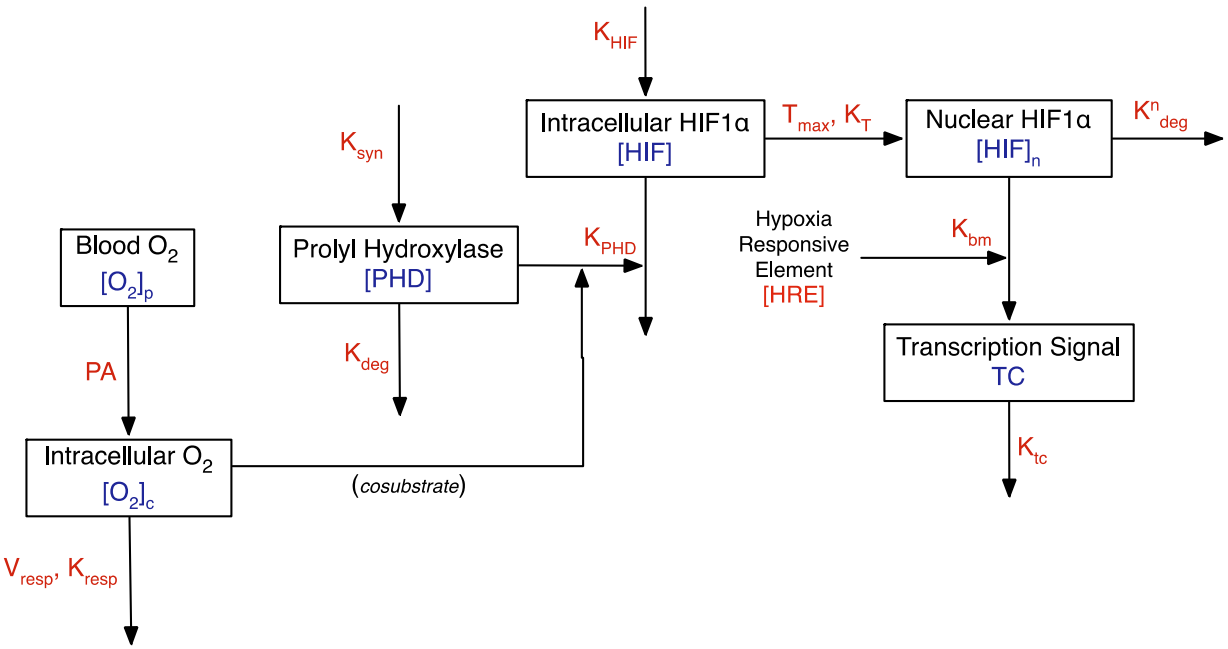

Figure 6. Schematic Representation of the Kinetic Model. Components whose concentration time course is modeled in response to changes in blood oxygen levels are shown in blue, while parameters or fixed values, that ultimately need to be experimentally determined, or fitted, are in red. For definitions of terms and abbreviations see text.

Briefly, the model assumes that oxygen movement from the blood into the intracellular space is determined by a permeability-surface area (*PA*) product. Once in the cell, it is removed via respiration at a maximum (saturable) rate for cell metabolism V_{resp}. Intracellular PHD levels are determined by the combined effect of synthesis (first order rate K_{syn}) and (constant, first-order) degradation of the enzyme K_{deg}. PHD hydroxylates HIF-1α, with intracellular levels of O_2 as a co-substrate (Semenza, 2004), and HIF-1α levels are determined from a balance of a constant zero order synthesis rate K_{hif}, and a PHD-dependent second-order degradation rate K_{phd}.

In addition, HIF-1α is transported into the nucleus, where it impacts gene expression. We assume a maximum transport rate T_{max}, and a half-saturation concentration of K_T.

The equations describing O_2, PHD and HIF-1α levels in the intracellular compartment (volume V_c) and the nucleus (volume V_n) are thus:

$$V_c \frac{d[O_2]_c}{dt} = PA.\left([O_2]_p - [O_2]_c\right) - \frac{V_{resp}.[O_2]_c}{K_{resp}+[O_2]_c} - K_{PHD}.[PHD].[HIF].[O_2]_c - \frac{T_{max}[HIF]}{[HIF]+K_T} \quad (1)$$

$$V_c \frac{d[PHD\}}{dt} = K_{syn} - K_{deg}.[PHD] \quad (2)$$

$$V_c \frac{d[HIF]}{dt} = K_{HIF} - K_{PHD}.[PHD].[HIF].[O_2]_c - \frac{T_{max}[HIF]}{[HIF]+K_T} \quad (3)$$

$$V_n \frac{d[HIF]_n}{dt} = \frac{T_{max}[HIF]}{[HIF]+K_T} - K_{deg}^n[HIF]_n - K_{bm}[HIF]_n[HRE], \quad (4)$$

where $[O_2]_p$ and $[O_2]_c$ are the concentrations (partial pressures) of oxygen in the plasma and cell intracellular compartments, [*PHD*] and [*HIF*] are the intracellular concentrations of prolyl hydroxylase and HIF-1α, respectively, and $[HIF]_n$ is the concentration of HIF-1α in the nucleus. Figure 6 shows a schematic of the model, with the modeled components in blue, and parameters or fixed values in red.

Once in the nucleus, HIF-1α is assumed to bind with HRE on the DNA with a bimolecular rate constant K_{bm}, and is degraded according to a first order rate constant K^n_{deg} (equation 4). The binding of HIF-1α to HRE initiates a transcription signal TC, which is assumed to mediate gene transcription. TC is assumed to decay spontaneously at a rate K_{tc}:

$$V_n \frac{dTC}{dt} = K_{bm}[HIF]_n[HRE] - K_{tc}.TC \quad (5)$$

These equations were incorporated into Berkeley Madonna™ (University of California, Berkeley CA) for the simulations that follow. Equations in the modelling language are contained in Appendix C.

4.0 RESULTS

4.1 *In Vitro* Results

The results of immunocytochemical staining for HIF-1α in the four cell lines were mixed. HIF-1α staining was observed in all cell lines at doses above 75 µM $CoCl_2$, but was most readily and consistently observed in SK-N-SH and C8-B4 cell lines (Figures 7 and 8, respectively). While the methods used were not quantitative, it appears that increasing concentrations of $CoCl_2$ lead to increasing activation of HIF-1α, nuclear condensation, cellular degradation and death, as expected in response to toxic exposures. Indications of toxicity complicates the interpretation of the HIF-1α results, since, among other things, synthesis of HIF-1α may be compromised as other mechanisms of Co toxicity become prevalent at high concentrations. In Figure 8, HIF-1α (red) is clearly co-localized with nuclei (blue), which is typical of the hypoxic response as HIF-1α is translocated to the nucleus and begins to influence gene expression.

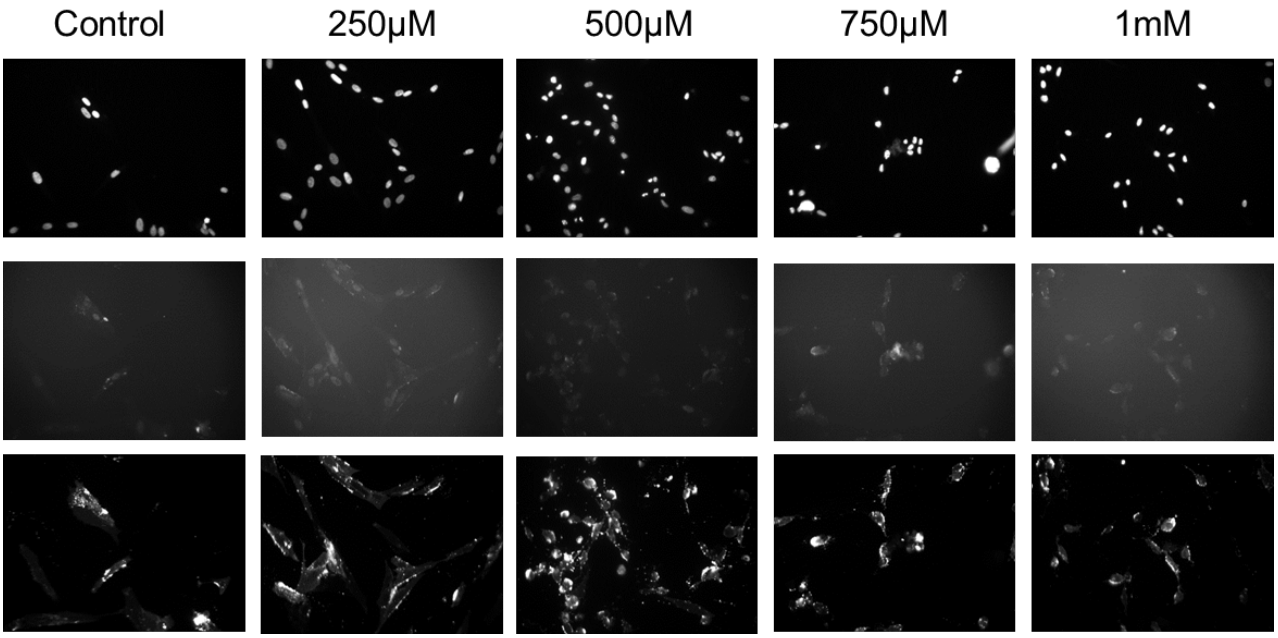

Figure 7. *In Vitro* Immunocytochemistry (ICC) on SK-N-SH cells under Mimicked Hypoxia ($CoCl_2$ Exposure). Top row shows nuclear staining, second row shows HIF-1α, and third row shows plasma membrane. Doses increase from control (far left) to 1mM $CoCl_2$ (far right). Exposure duration was 24 hours. All cells imaged at 20x magnification.

HIF-1α detection by ELISA revealed that after 24 hours of exposure to 250 µM $CoCl_2$, all of the cell lines had some HIF-1α activation above basal levels. The highest observed HIF-1α concentrations were in the SK-N-SH cell line, in the range of 1.6 to 4.5 pg/µg total protein. The other cell lines had much lower concentrations, in the range of 0.16 to 0.46 pg/µg total protein.

Important lessons were learned throughout the performance of this study. The two most important were:

- CellLight (Invitrogen) dyes were not effective for visualizing plasma membrane in NE-4C, N2a, and C8-B4 cell lines.
- Mass spectrometry was tested as an alternative method for the detection of HIF-1α in cell lysates, but it was determined that, even with use of an internal standard, this method was questionable. ELISA is a much more practical and economical method of detection.

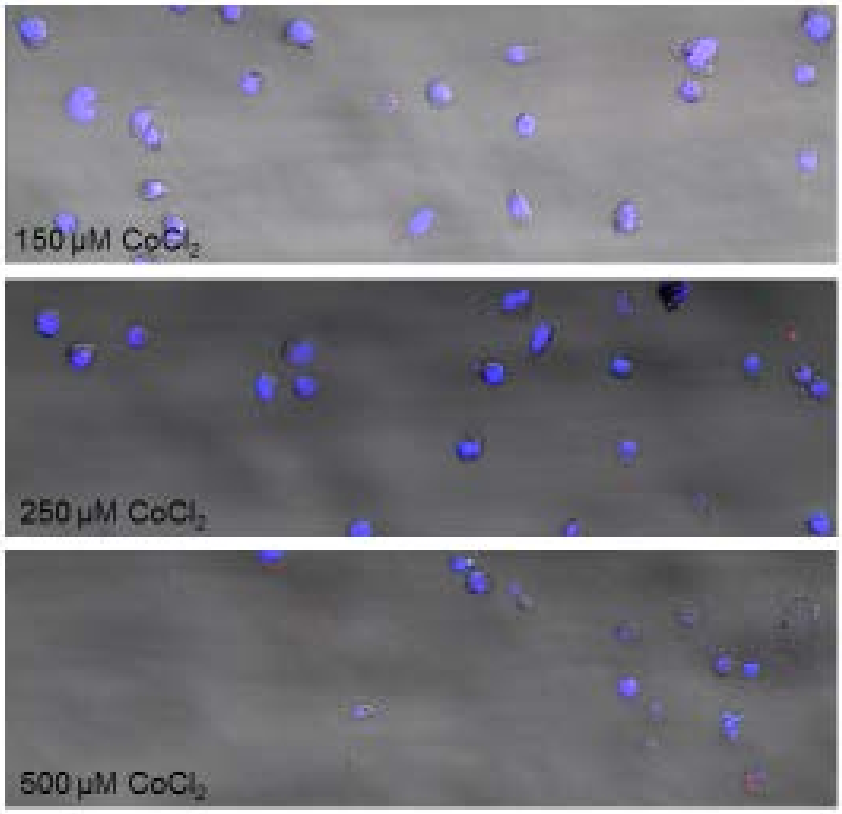

Figure 8. Nuclear Localization of HIF-1α at Low Doses of Hypoxia Mimetic, $CoCl_2$. HIF-1α shown in red, nuclei in blue. Cells fixed following 24-hour exposure. Note apparent cytotoxicity at 500 µM dose. Cells imaged at 20x magnification.

4.2 Hypoxia Chamber Results

The HIF-1α ELISA demonstrated induction in the SK-N-SH neuronal cell line as shown in Figure 9. This is consistent with a previous report in the literature where HIF-1α was increased under hypoxic states induced in a neuroblastoma cell line (Foti *et al.*, 2010). The successful induction of HIF-1α expression confirmed that the gas chamber and lumox® plates provided a platform to expose *in vitro* cell models to hypoxic conditions and study changes at the molecular level.

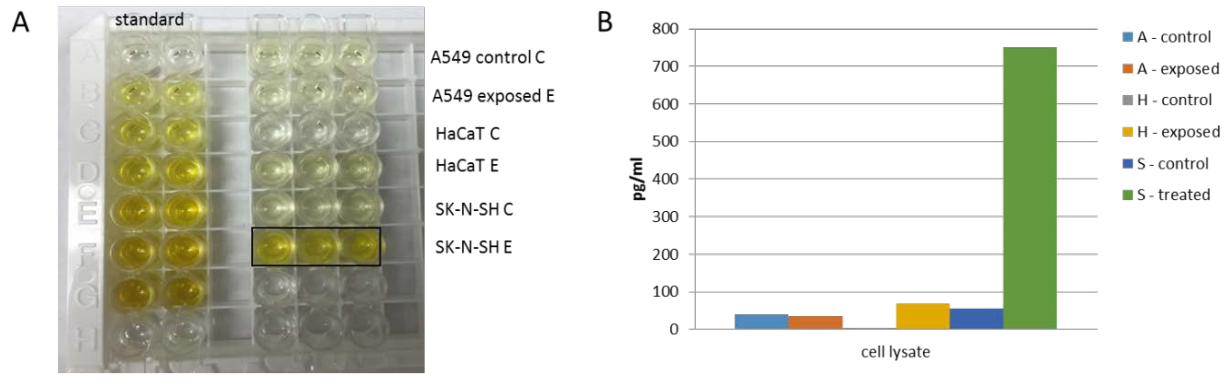

Figure 9. Quantifying Induction of HIF-1α Expression using ELISA. A) HIF-1α ELISA plate layout; B) HIF-1α induction (pg/ml) in three different cell models where A = A549; H = HaCaT; and S = SK-N-SH. The A549 and HaCaT cell lines did not demonstrate increased expression of HIF-1α following 2-hour exposure to hypoxic conditions. The SK-N-SH cell line revealed increases in HIF-1α expression.

4.3 Mathematical Simulations

Figure 10 shows the results of a sample simulation in which normal oxygen concentrations are reduced, at time t = 2, from 100 mmHg to a value still within the normal range of 80 to 105 mmHg ($[O_2]_p$ = 90 mmHg), and a value representative of hypoxia ($[O_2]_p$ = 55 mmHg). Chemical concentrations and time are in arbitrary units. Note that both HIF-1α and PHD concentrations in the cell compartments eventually reach a steady-state, given by setting equations (2), (3) and (4) to zero.

Simulations such as these can be used to describe and interpret experimental data in terms of underlying mechanisms. Such experiments, if quantitative, can also be used to calibrate and parameterize the model. For example, Figure 5 shows preliminary *in vitro* immunocytochemistry (ICC) on cells under mimicked hypoxia ($CoCl_2$ exposure). More data like these, collected and quantified at different times so as to characterize the time-course of HIF-1α accumulation in the cytoplasm and its subsequent translocation into the nucleus, can be used to estimate changes in PHD-dependent second-order degradation rate K_{phd} of HIF-1α, and to estimate parameters for HIF-1α transport into the nucleus, respectively. These empirically determined values can then be added to the HIF-1α model to improve application in real-world scenarios.

The model can also be used to simulate a finite period of hypoxia, followed by return to normoxia (step function) (Figure 11). Finally, the model can produce predictions of behavior under repeated (chronic) intermittent hypoxia conditions (Figure 12). Note that under certain conditions, there is a tendency for the transcription signal not to return to its baseline value between exposures, because of insufficient time.

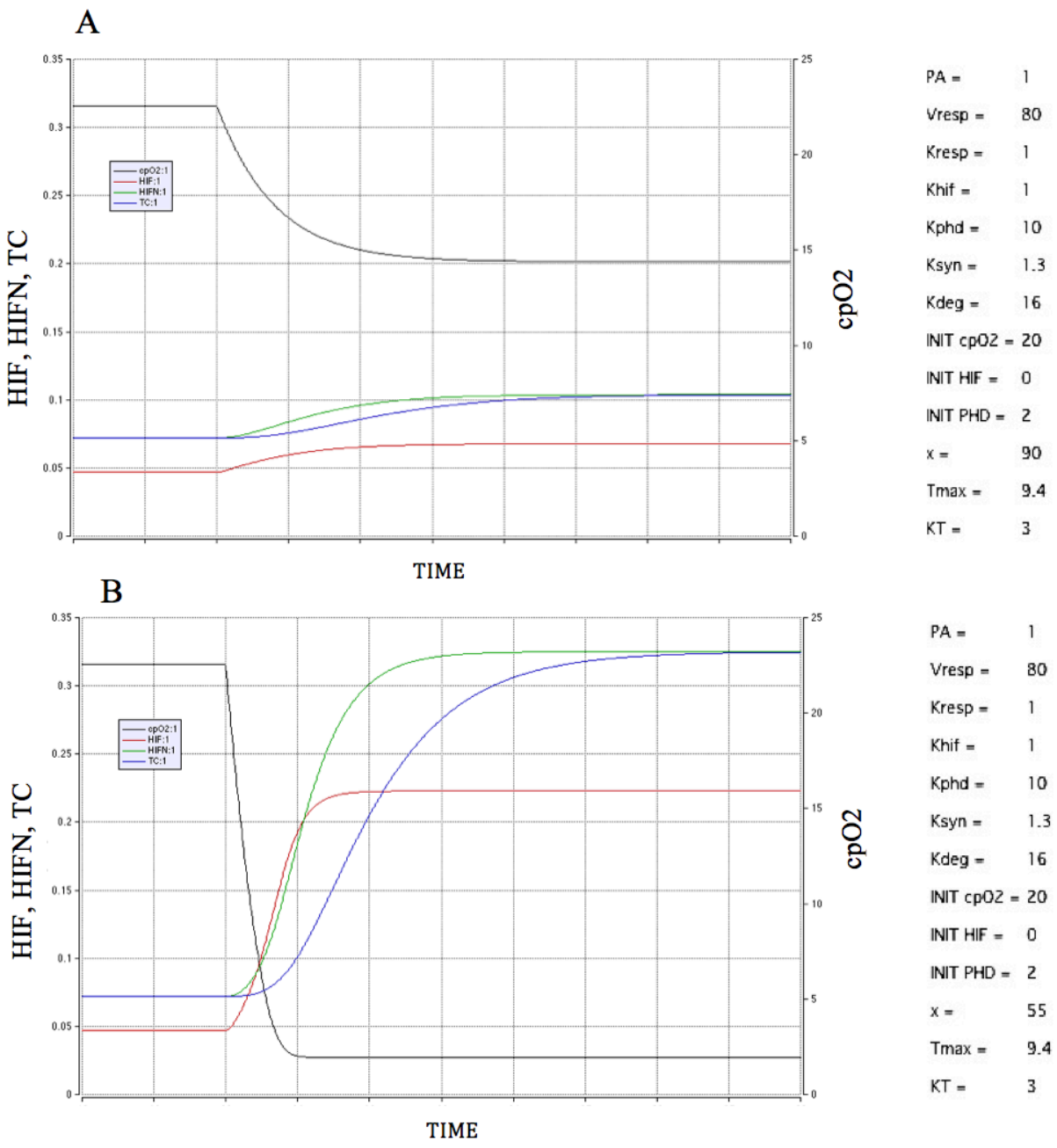

Figure 10. Simulation Outputs from HIF-1α Kinetic Model. The simulations show the effect of reduction of the partial pressure of oxygen in the blood from a normal value of 100 mmHg, to 90 mmHg (A) and 55 mmHg (B), on intracellular oxygen tension (cpO_2, black line) and the consequent increase in HIF-1α due to reduction in O_2-dependent prolyl hydroxylase (PHD) activity, both in the cytosol (HIF, red line) and in the nucleus (HIFN, green line). The blue line shows the resulting predicted transcription signal TC. Both concentrations and time are in arbitrary units.

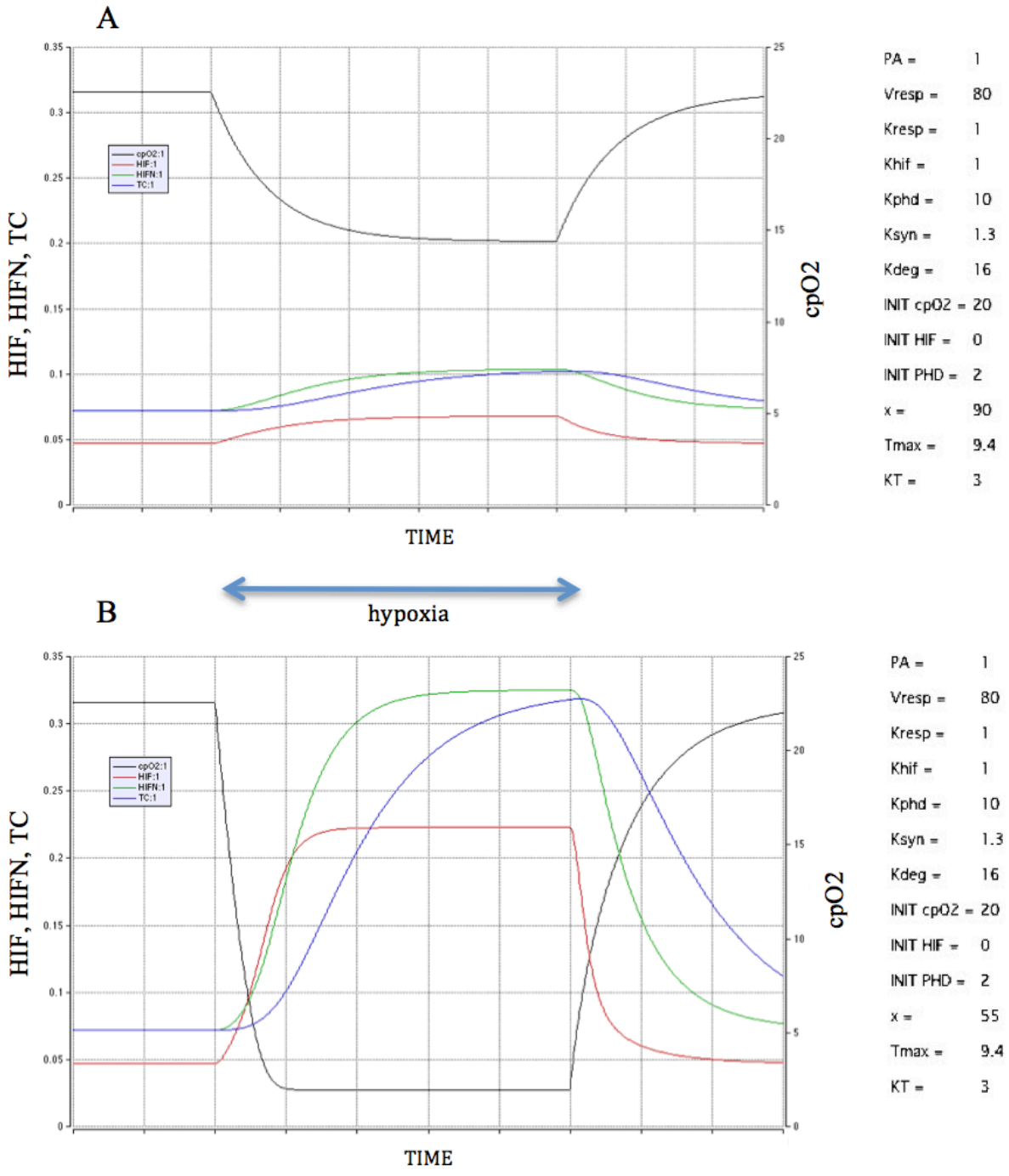

Figure 11: Simulations of Return to Normoxia. Conditions are the same as in Figure 10. Both concentrations and time are in arbitrary units.

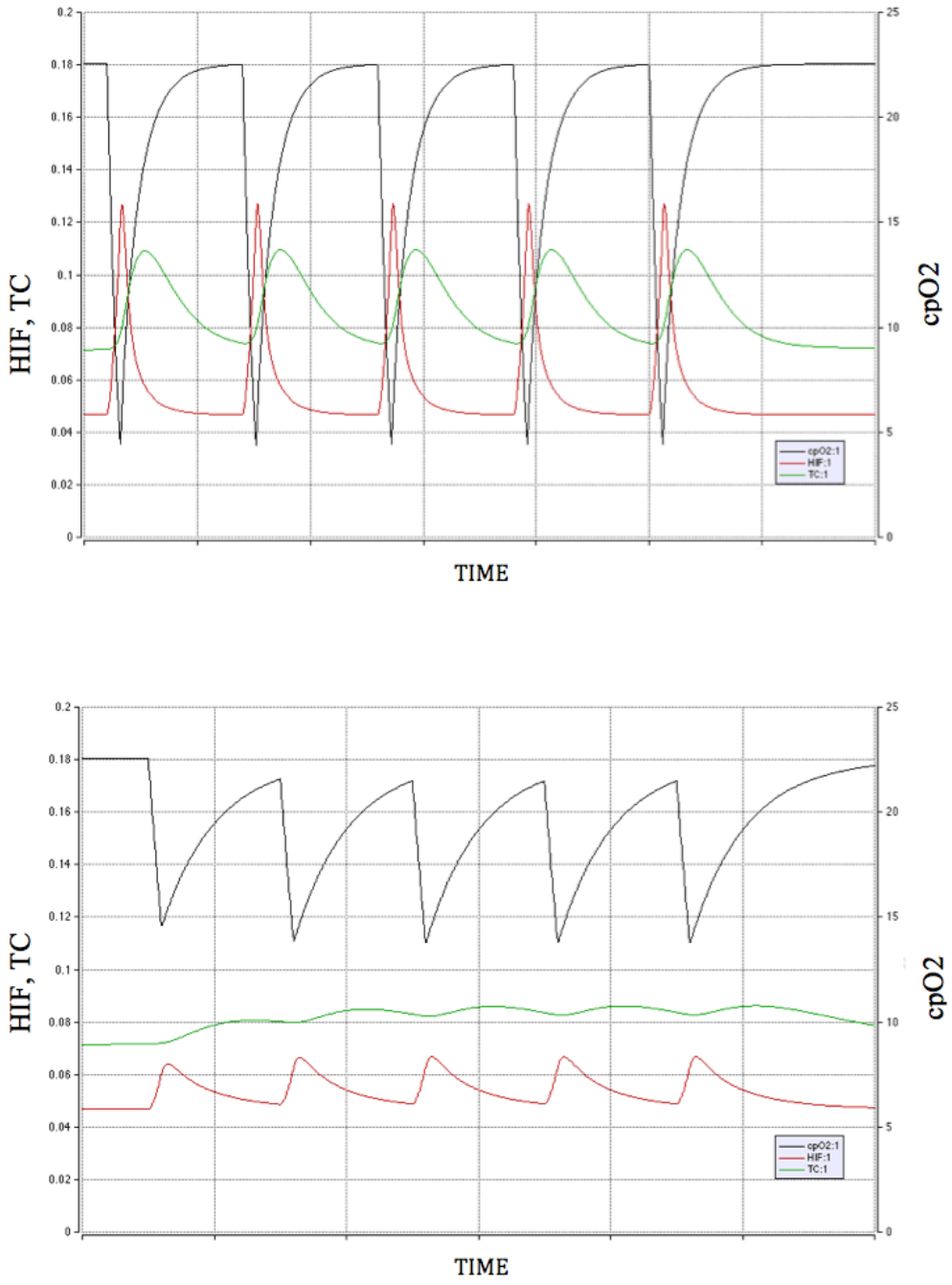

Figure 12. Simulations of Repeated Intermittent Hypoxia. Hypoxic episodes are equivalent to 10 percent of the total time. The simulations show the effect of length of periods of hypoxia on cellular oxygen levels (cpO_2, top curve), intracellular HIF-1α levels (HIF, bottom curve) and transcription signal (TC, middle green curve). The oxygen concentration in the blood is reduced intermittently from a normal value of 90 mmHg, to 55 mmHg in each case; the difference is that in the bottom graph the cycle time is three times shorter, resulting in a tendency for the transcription signal not to return to its baseline value between exposures. Both concentrations and time are in arbitrary units.

5.0 CONCLUSIONS AND FUTURE WORK

5.1 *In Vitro* Studies

One of the risks associated with this study results from the use of $CoCl_2$ as a surrogate for true hypoxic exposure. It is unknown whether the signaling cascade and downstream molecular activities are the same when cells are exposed to $CoCl_2$ rather than a low-O_2 environment. It is also impossible to correlate $CoCl_2$ dosage with real-world hypoxic exposure. So, while this study did show that we can visualize the activation of HIF-1α *in vitro* using ELISA and immunocytochemistry, it did not reveal any new information about the hypoxia pathway, or any new targets for exploration either *in vivo* or *in vitro*. Future studies simulating hypoxic exposure of cells in the custom atmospheric exposure chamber could be performed, followed by downstream molecular, proteomic, and immunocytochemical studies. This approach using the chamber may reveal new information about the hypoxic response and provide targets for further exploration in *in vivo* studies.

5.2 Hypoxia Chamber Studies

Three different human cell lines representing the lung epithelium (A549), keratinocytes (HaCaT), and neurons (SK-N-SH) were grown under hypoxic conditions (1 percent O_2) to determine expression changes for HIF-1α. When a polystyrene 24-well plate with cells was exposed to gas or vapor, cells adhered on the bottom of the well were not exposed to vapor due to a liquid barrier created by the medium which caused slow equilibrium diffusion between the medium and gas phase. To overcome this obstacle, lumox® plates were employed. Cells adhered to the bottom of the lumox® plate, which is a thin film and readily allows for gas exchange at the cell surface. Following a 2 hour exposure to 1 percent O_2, the cells were lysed and protein was extracted to determine HIF-1α expression. Among the three cell lines tested, the neuronal cells demonstrated a significant increase in HIF-1α expression due to a hypoxic state, which is consistent with the findings from a previous study reported in the literature (Foti *et al.*, 2010) and validated the use of the chamber to achieve hypoxic cell exposures. The fact that HIF-1α was not detected in all three cell lines may indicate that longer exposure times or lower oxygen concentrations are necessary in order to induce a hypoxic response in A549 and HaCaT cell lines.

5.3 Model Parameterization and Further Development

The current model, shown schematically in Figure 6 and described by equations (1) through (5), has limitations. Firstly, the parameters used in the model are largely arbitrary, and chosen to allow the model to exhibit the desired behavior. Analysis of the literature will allow some of the relevant parameters to be determined. For example, prolyl hydroxylases have a K_m value for O_2

that is slightly above its atmospheric concentration, such that O_2 is rate limiting for enzymatic activity under physiological conditions. As a result, changes in the cellular O_2 concentration are directly transduced into changes in the rate at which HIF-1α is hydroxylated, ubiquitinated, and degraded (Semenza, 2004). In addition, some potentially important and quantifiable pathways are not yet incorporated into the model. For example, factor inhibiting HIF-1 (FIH-1), which inhibits the activity of the HIF-1α transactivation domain, functions as the asparaginyl hydroxylase, and has a K_m for O_2 that is three times lower than the prolyl hydroxylases. Asparagine hydroxylation prevents the interaction of HIF-1α with the coactivators CBP and p300 (see Figure 2 above).

The current model describes cellular regulation of HIF-1α in response to hypoxia, and in order to describe the response of the organism as a whole, it needs to be extended, and linked with models of upstream processes such as the delivery of oxygen to the tissue, and downstream processes involving the modulation of specific biological pathways by HIF-1α mediated gene transcription, such as angiogenesis. In such an extended model, for example, the output from the current model (HIF-1α binding to the HRE and the resulting transcription signal) would provide an input to a model of gene expression such as those published by Chen et al. (1999) or Ay et al. (2011). For example, Chen et al. (1999) developed a differential equation based model to describe gene expression based on Figure 13. Here HIF-1α binding to the gene (DNA) is shown in red.

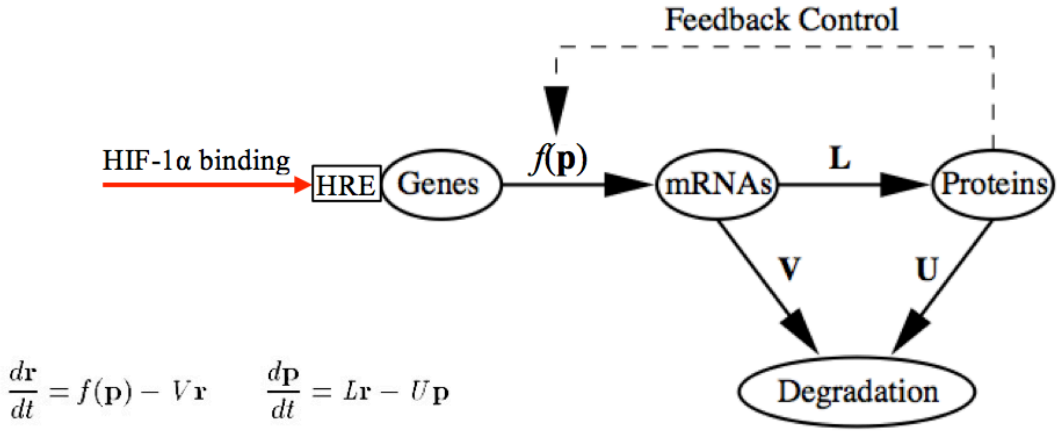

Figure 13. Schematic of a Simple Differential Equation Based Model of Gene Expression. Based on Chen *et al.* (1999).

It is in the adaptive and deleterious effects of longer term and intermittent exposure to hypoxia (and hyperoxia) mediated by gene transcription where we see the greatest potential for adaptation and negative health effects. Longer term results of gene expression include angiogenesis and apoptosis. Gene transcription is linked with cortical capillary density, both as a result of hypoxia (angiogenesis) and return to normoxia (or hyperoxia) (apoptosis). For example, the protein VEGF (vascular endothelial growth factor) is upregulated by HIF-1α, and is responsible for angiogenesis. HIF-1α levels during 21 days of hypoxia are shown in Figure 14A. Since tissue diffusion distance is a key parameter for oxygen delivery to tissue, it is the ratio of oxygen tension in the blood to intercapillary distance that is the (longer term) parameter responsible for mediating hypoxic/normoxic/hyperoxic changes. Thus, chronic exposure to hypoxia leads to structural and functional changes. For example, over a period of 1 to 3 weeks following hypoxic exposure in rats, a doubling of the capillary density, leading to a decrease in intercapillary distances, has been observed (Pichiule and LaManna, 2002; see Figure 14B). These changes are reversible upon restoration of normal ambient oxygen concentrations, again over a 3 week period. Capillary regression is mediated by apoptosis. "The implication from these observations is that the brain naturally functions in a low, but controlled, oxygen environment. Acute imbalances in oxygen delivery and metabolic demand are addressed through changes in blood flow; persistent imbalances activate mechanisms that adjust capillary density" (Pichiule and LaManna, 2002).

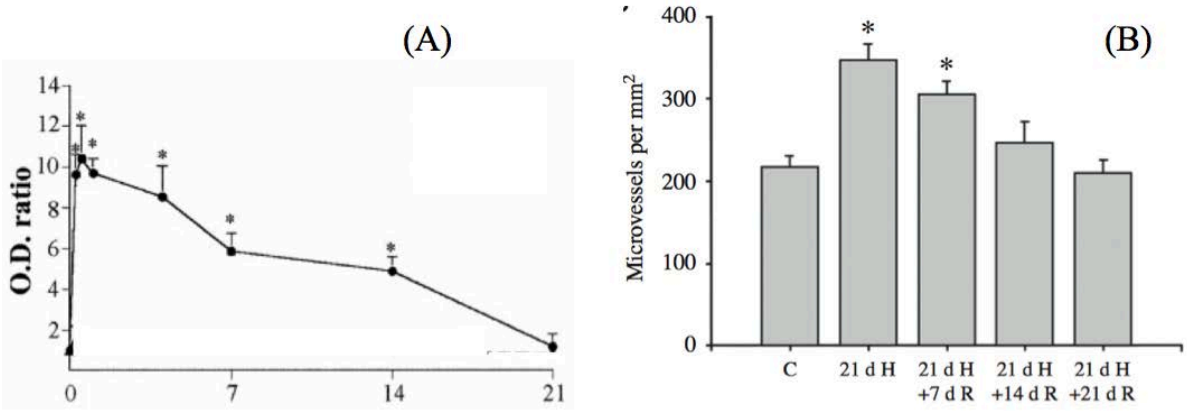

Figure 14. Chronic Hypoxia Effects. (A) HIF-1α measured in the cortex of rats exposed to hypoxic conditions for 6 hours to 21 days, relative to normoxic controls (0.5 atmospheres, equivalent to 10 percent normobaric oxygen) (Chavez *et al.*, 2000). (B) Photomicrographs of GLUT-1- stained sections indicate that capillary density in the rat cerebral cortex increased by 60 percent after 3 weeks of hypoxia (0.5 atmospheres, equivalent to 10 percent normobaric oxygen) and that it progressively decreased to prehypoxic values after 3 weeks of normoxic recovery (adapted from Pichiule and La Manna 2002).

Application of the HIF-1α model to the carotid body is speculative (see Section 2.0). However, hydroxylation of HIF-1α in the presence of O_2 occurs in a few minutes; hence it is conceivable that O_2-dependent hydroxylases could also modulate ion channels and thus participate in the acute responses to hypoxia (Lopez-Barneo *et al.*, 2008). If we assume that oxygen sensing is again mediated by the intracellular levels of HIF-1α, then we have the scheme outlined in Figure 15.

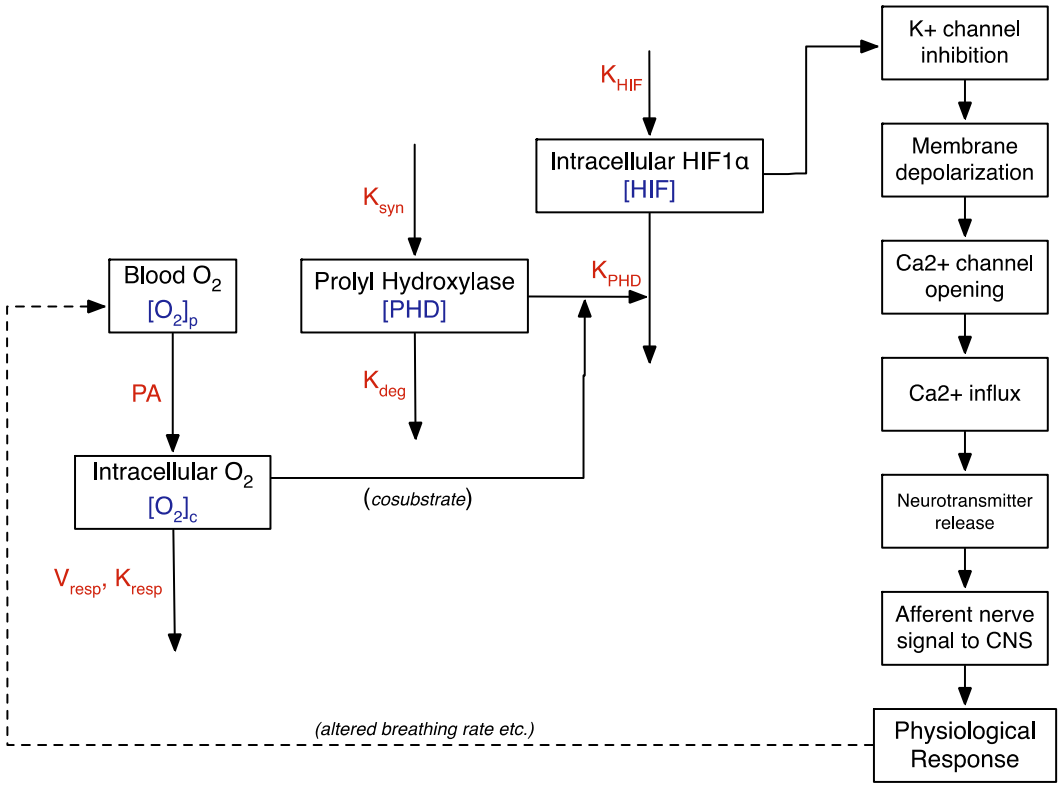

Figure 15. Schematic of a Potential Model for Oxygen Sensing in the Carotid Body

Additional rapid response pathways potentially mediated, at least in part, by the HIF-1α pathway, include nitric oxide synthase (NOS) activation (Jung *et al.*, 2000), vasodilation, glucose transport, and metabolism. Control of cerebral blood flow is complex and only partially understood. Relevant processes include cerebral pressure autoregulation, which maintains a constant flow despite changing cerebral perfusion pressure. The brain is also able to vary blood flow to match metabolic activity (flow-metabolism coupling). Finally, a network of perivascular nerves also serves to regulate cerebral blood flow (neurogenic regulation) (Peterson *et al.*, 2011).

Input to the HIF-1α model *in vivo* comes from blood oxygen levels, and the model can be linked to a whole body oxygen delivery model. Many such models, at various levels of physiological detail, are available in the literature. For example, Topor *et al.* (2004) have developed a mathematical model which describes multiple mechanisms associated with control of breathing in response to hypoxia. In addition to hypoxic conditions, ambient pressures and air quality also

potentially add to the impact of hypoxia on physiological responses. In many cases oxygen delivery issues are concurrent with ambient diverse chemical exposure issues. For example, as mentioned in the *Introduction*, toluene is a known contamination component that comes through the aircraft's on-board oxygen generation system, and may potentially impact oxygen delivery (Martin *et al.*, 2012). Previous in-house experiments have investigated the effect of altitude on the distribution of toluene in rats by providing a better understanding of how these stressors affect the brain at the cellular and molecular level. Ongoing studies with toluene combined with hypoxia are investigating the effects of altitude, chemical exposure and altered percentage of oxygen on the function of neural cells in the brain by measuring changes in the electrical patterns of brain cells. Toluene also may potentially interact with hemoglobin, altering its binding characteristics and thereby the oxygen carrying capacity of the blood (Chushak *et al.*, 2015).

In summary, these projects lay the foundation for future *in vitro* and *in vivo* investigations into the role of HIF-1α on the molecular level, and the impact of hypoxia in animal models. Future mechanistic and kinetic studies, in combination with a thorough review of existing literature, will enable parameterization of the HIF-1α model and eventual extrapolation to relate these data to pilots of high-performance aircraft.

6.0 REFERENCES

Ay, A., Arnosti, D. N. (2011). Mathematical modeling of gene expression: a guide for the perplexed biologist. Crit. Rev. Biochem. Molec. Biol. 46(2), 137–151.

Chavez, J. C., Agani, F., Pichiule, P., Lamanna, J. C. (2000). Expression of hypoxia-inducible factor-1 alpha in the brain of rats during chronic hypoxia. J. Appl. Physiol. 89, 1937–1942.

Chen, T., He, H. L., Church, G. M. (1999). Modeling gene expression with differential equations. Pac. Symp. Biocomput. 1–12.

Chushak, Y. G., Chapleau, R. R., Frey, J. S., Mauzy, C. A., Gearhart, J. M. (2015) Identifying potential protein targets for toluene using molecular similarity search, *in silico* docking and *in vitro* validation. Toxicol. Res. 4, 519-526.

Foti, R., Zucchelli, S., Biagioli, M., Roncaglia, P., Vilotti, S., Calligaris, R., Krmac, H., Girardini, J. E., Del Sal, G., Gustincich, S. (2010). Parkinson disease-associated DJ-1 required for the expression of the glial cell line-derived neurotrophic factor receptor RET in human neuroblastoma cells. J. Biol. Chem. 285, 18565-18574.

Jung, F., Palmer, L. A., Zhou, N., Johns, R. A. (2000). Hypoxic regulation of inducible nitric oxide synthase via hypoxia inducible factor-1 in cardiac myocytes. Circ. Res. 86(3), 319–325.

Kline, D. D., Peng, Y., Manalo, D. J., Semenza, G. L., Prabhakar, N. R. (2002) Defective carotid body function and impaired ventilatory responses to chronic hypoxia in mice partially deficient for hypoxia-inducible factor 1α. Proc. Natl. Acad. Sci. USA, 99, 821–826.

LaManna, J. C., Chavez, J. C., Pichiule, P. (2004). Structural and functional adaptation to hypoxia in the rat brain. J. Exper. Biol. 207(Pt 18), 3163–3169.

López-Barneo, J., Ortega-Sáenz, P., Pardal, R., Pascual, A., Piruat, J. I. (2008). Carotid body oxygen sensing. Eur. Respir. J. 32(5), 1386–1398.

Martin, G., Muellner, G., Anderson, J., Brinkley, J., Delaney, L., Demitry, P., Moore, D, Moorman, T. (2012). Report on Aircraft Oxygen Generation. Washington, D.C.: United States Air Force Scientific Advisory Board. SAB-TR-11-04, 1 February 2012.

Peng, Y., Yuan, G., Ramakrishnan, D., Sharma, S. D., Bosch-Marcé, M., Kumar, G. K., Semenza, G. L., Prabhakar, N. R. (2006) Heterozygous HIF-1α deficiency impairs carotid body-mediated systemic responses and reactive oxygen species generation in mice exposed to intermittent hypoxia. J. Physiol. 577, 705–716.

Peterson, E. C., Wang, Z., Britz, G. (2011). Regulation of cerebral blood flow. Int. J. Vasc. Med., Epub 2011, July 25, Article ID 823525, doi: 10.1155/2011/823525

Pichiule, P., LaManna, J. C. (2002). Angiopoietin-2 and rat brain capillary remodeling during adaptation and deadaptation to prolonged mild hypoxia. J. Appl. Physiol. 93(3), 1131–1139.

Prabhakar, N. R. (2013). Sensing hypoxia: physiology, genetics and epigenetics. J. Physiol. 591(Pt 9), 2245–2257.

Semenza, G. L. (2004). Hydroxylation of HIF-1: oxygen sensing at the molecular level. Physiology, 19, 176–182.

Topor, Z. L., Pawlicki, M., Remmers, J. E. (2004). A computational model of the human respiratory control system: responses to hypoxia and hypercapnia. Ann. Biomed. Eng. 32(11), 1530–1545.

Wyatt, Christopher N., Ph.D., Interim Chair and Associate Professor; Neuroscience, Cell Biology, and Physiology; Wright State University, Dayton, OH.

Yu, K. O., Meade, M. L., Capati, R. H., Schlager, J. J., Mattie, D. R., James, R. A., Ray, M. J., Dixon, D. A., Braydich-Stolle, L. K., Sterner, T. R., Hoffmann, A. (2015). Toluene Dose-Response and Preliminary Study of Proteomics for Neuronal Cell Lines. Wright-Patterson AFB OH: Air Force Research Laboratory, 711th Human Performance Wing, Human Effectiveness Directorate, Bioeffects Division, Molecular Bioeffects Branch. AFRL-RH-WP-TR-2015-0086.

Yuan, Y., Hilliard, G., Ferguson, T., Millhorn, D. E. (2003). Cobalt inhibits the interaction between hypoxia-inducible factor and von Hippel-Lindau protein by direct binding to hypoxia-inducible factor. J. Biol. Chem. 278(18), 15911–15916.

APPENDIX A. CELL RECOVERY AND LYSIS PROCEDURE

Cell Recovery from lumox® plates

1. Immediately after exposure, carefully scrape the cells (n=8) in original medium not to damage bottom of the thin film (50 µm thickness) at RT.
    a. When the cells were scraped in cold condition, portion of thin film at the bottom was detached, and the contents were leaked out. It could be due to cold condition since polystyrene frame and thin film would have different rate of shrinking at the cold condition.
2. Transfer cell suspension from 8 wells of same cell lines into a 15 mL tube (total volume <4 mL) in ice. Add 0.5 mL cold PBS into each well (n=8), and scrape carefully, and transfer PBS into the same tube. Total volume would be ~8 mL. Spin the cell suspension at 1000xg for 5 minutes.
3. Remove supernatant, and add 3 mL cold PBS to wash cell pellets.
4. Vortex and spin 1000xg for 5 minutes.
5. Remove PBS, and add 1 mL cold PBS, vortex, and transfer cell suspension into 1.5 mL tube. Spin 1000xg for10 minutes, and remove as much PBS as possible.
6. Repeat this process for all cells (exposed and control). There will be 6 tubes.

Cell Lysis

1. Solubilize cells at $1x10^7$ cells/mL in Lysis Buffer #11 and allow samples to sit on ice for 15 minutes.
2. To clarify the lysates, centrifuge samples at 2000xg for 5 minutes and transfer the supernatant to a clean test tube.
3. Aliquot 10-15 µL of the lysate for protein determination.
4. Store clarified lysates at ≤-70°C.

Lysis Buffer #11

Reagent	MW or [Initial]	[Final]	Buffer Vol (mL)	Amt Reagent	Unit	
NaCl	58.44 g/mole	300 mM	12.5	0.219	g	
EDTA	0.5 M	3mM	12.5	0.075	mL	
MgCl2	203.3 g/mole	1 mM	12.5	0.00255	g	
β-Glycerophosphate	216.04 g/mole	20 mM	12.5	0.054	g	
NaF	41.99 g/mole	25 mM	12.5	0.0131	g	
Glycerol		10% w/v	12.5	1.25	mL	
Triton X-100		0.01	12.5	0.0125	mL	
Leupeptin (10mg/mL)		25 µg/mL	12.5	31.25	µL	
Pepstatin (5mg/mL)		25 µg/mL	12.5	62.5	µL	
Aprotinin		3 µg/mL	12.5	18.8	µL	
Tris	121.14 g/mole	50 mM	12.5	0.076	g	
Water			12.5	11.05	mL	
			Adjust pH to 7.4			

APPENDIX B. HIF-1α ELISA PROCEDURE

The Human/Mouse Total HIF-1α ELISA was purchased from R&D Systems and the manufacturer's recommended protocol was optimized using the following procedure.

Day 1: Plate Preparation

1. Prepare 1L of 1X PBS
2. Prepare 1L of 0.05% Tween-20 in 1X PBS (= Wash Buffer)
3. Prepare 100 mL of 5% bovine serum albumin (BSA) in Wash Buffer (5 g BSA into 100 mL Wash Buffer = Reagent Diluent)
4. Prepare Stop Solution by adding 2.7 mL concentrated H_2SO_4 to 47.3 mL H_2O = 1M or 2N solution.
5. Dilute the Capture Antibody to the working concentration of 4.0 µg/mL in PBS without carrier protein. (Re-suspend CA in 200 µL PBS = 720 µg/mL; Add 59 µL CA solution to 10.541 mL PBS.) Immediately coat a 96-well microplate with 100 µL per well of the diluted Capture Antibody. Seal the plate and incubate overnight at room temperature.

Day 2:

1. Aspirate each well and wash with 400 µL Wash Buffer, repeating the process two additional times for a total of 3 washes. After the last wash, remove any remaining Wash Buffer by aspirating or by inverting the plate and blotting it against clean paper towels.
2. Block plates by adding 300 µL of Reagent Diluent to each well. Incubate at room temperature for 1-2 hours.
3. Repeat the aspiration/wash as in step 1 above.
4. Add 100 µL of sample or standards in Reagent Diluent per well. Use Reagent Diluent as the zero standard. Cover with a plate sealer and incubate 2 hours at room temperature.
    a. Standard curve preparation: A seven point standard curve using 2-fold serial dilutions and a high standard of 8,000 pg/mL is recommended. First, dilute standard 22.5X (30µL into 645µL RD), then transfer 300µL of this solution to a tube containing 300 µL RD. Repeat 4X to obtain standards: 8,000; 4,000; 2,000; 1,000; 500; 250 pg/mL.
5. Dilute the Detection Antibody (DA) to a working concentration of 100 ng/mL in Reagent Diluent before use. Re-suspend DA in 1 mL of RD = 3.6 µg/mL. Transfer 294 µL of DA solution into a tube containing 10.306 mL RD = 100 ng/mL.
6. Repeat the aspiration/wash as in step 1 above.
7. Add 100 µL of the diluted Detection Antibody to each well. Cover with a new plate sealer and incubate 2 hours at room temperature.
8. Repeat the aspiration/wash as in step 1 above.
9. Immediately before use, dilute the Streptavidin-HRP to the working concentration specified on the vial label using Reagent Diluent. (Pipet 53 µL of supplied Streptavidin-HRP into 10.547 mL RD = 1:200 dilution.) Add 100 µL of the diluted Streptavidin-HRP to each well. Incubate for 20 minutes at room temperature. Avoid placing the plate in direct light.
10. Repeat the aspiration/wash as in step 1 above.

11. Warm Tetramethylbenzidine to room temperature immediately before use. Add 100 µL of this Substrate Solution to each well. Incubate for 20 minutes at room temperature. Avoid placing the plate in direct light.
12. Add 50 µL of Stop Solution to each well. Gently tap the plate to ensure thorough mixing.
13. Determine the optical density of each well immediately, using a microplate reader set to 450 nm. If wavelength correction is available, set to 540 nm or 570 nm. If wavelength correction is not available, subtract readings at 540 nm or 570 nm from the readings at 450 nm. (This subtraction will correct for optical imperfections in the plate.)

APPENDIX C. HIF-1α MODEL (BERKELEY MADONNA)

```
METHOD RK4

STARTTIME = 0
STOPTIME=60
DT = 0.02

bpO2 = IF TIME <= 20 OR TIME >=40 THEN 100 ELSE x
x=50 ; reduced bpO2
;d/dt(bpO2) = 0

Vc*d/dt(cpO2) = PA*(bpO2 - cpO2) - Vresp*cpO2/(Kresp+cpO2)

Vc*d/dt(HIF) = Khif - Kphd*PHD*HIF - Tmax*HIF/(HIF+KT)

Vn*d/dt(HIFN) = Tmax*HIF/(HIF+KT) - KdegN*HIFN - Kbm*HIFN*HRE

Vn*d/dt(TC) = Kbm*HIFN*HRE - Ktc*TC

Vc*d/dt(PHD) = Ksyn*cpO2 - Kdeg*PHD

;init bpO2 = 100; mmHg, pO2 in blood. normal range (human) is 80-105 mmHg
init cpO2 = 20;  mmHg, pO2 in the cell
init HIF = 0; HIF1alpha
init PHD = 5; prolyl hydroxylase
init HIFN = 0 ; HIF1alpha in nucleus
init TC = 0; transcription signal due to binding of nuclear HIF1alpha with HRE

PA = 1; permeability area cross product for O2
Vresp = 80; max rate of respiration (removal of O2)
Kresp = 1; O2 at half-max respiration
Khif = 1; 0-order synthesis of HIF
Kphd = 0.2; bimolecular degradation of HIF by PHD
Ksyn = 1.3; O2 dependent synthesis of PHD
Kdeg = 16; 1st order degradation of PHD
KdegN = 1; 1st order degradation of HIF1alpha in the nucleus
Kbm = 1; bimolecular rate constant for binding of HIF1alpha to HRE - hypoxia responsive
element - in the nucleus
HRE=1
Ktc=1
Vc=1; volume of intracellular compartment
Vn=1; volume of nucleus
Tmax=1; Transport to nucleus (max)
KT=10; Km for transport to nucleus29
HIF-1α
```

LIST OF ACRONYMS

A549	adenocarcinomic alveolar basal epithelial cells A549
ATCC	American Type Culture Collection
BSA	bovine serum albumin
C8-B4	transformed mouse cerebellum microglial cells C8-B4
CB	carotid body
CBP	cAMP response element binding protein
$CoCl_2$	cobalt chloride
DA	detection antibody
EDTA	ethylenediaminetetraacetic acid
ELISA	enzyme-linked immunosorbent assay
EMEM	Eagle's minimum essential medium
FBS	fetal bovine serum
FIH	factor inhibiting hypoxia inducing factor
HaCaT	transformed aneuploid immortal keratinocyte cells HaCaT
HIF	hypoxia inducing factor
HIFN	hypoxia inducing factor in the nucleus
HRE	hypoxia responsive element
ICC	immunocytochemistry
IHC	immunohistochemical staining
N2a	mouse neuroblastoma cells N2a
NE-4C	mouse embryonic neuroectodermal stem cells NE-4C
NOS	nitric oxide synthase
OBOGS	on-board oxygen generation system
PA	permeability area cross product
PHD	prolyl hydroxylase
SK-N-SH	human neuroblastoma cells
TAD	transactivation domain
TC	transcription signal
VHL	von Hippel-Lindau tumor suppressor protein